

\mathcal{H}_2 Optimization Applied to General Transmultiplexer Design¹

Ting Liu

Dept. of Elect. & Comp. Eng.
Queen's University
Kingston, Ontario
Canada K7L 3N6

Tongwen Chen²

Dept. of Elect. & Comp. Eng.
University of Alberta
Edmonton, Alberta
Canada T6G 2G7

Abstract

The paper considers design of multi-channel, nonuniform-band transmultiplexers using \mathcal{H}_2 optimization. General dual-rate structures are used to provide more design freedom. Such general transmultiplexers have a new source of error called *aliasing distortion*. We propose a composite error criterion which captures all distortions in one, develop an optimal design procedure and apply it to a three-channel nonuniform example, yielding an FIR transmultiplexer which has good frequency limiting properties in the synthesis end and is very close to perfect reconstruction.

1 Introduction

Typical studies of transmultiplexers focus on uniform-band structures in which incoming data signals are assumed to have the same sampling rate and are upsampled at the same integer factor. In this paper, our goal is to study nonuniform transmultiplexers where incoming signals have possibly different sampling rates and thus are upsampled at different fractional ratios.

A general nonuniform transmultiplexer built with general blocks is shown in Figure 1. For well designed transmultiplexers, \hat{x}_i approximates x_i . Ideally, we say the transmultiplexer achieves *perfect reconstruction* [7, 6] if \hat{x}_i is a delayed version of x_i , namely, if there exist nonnegative integers d_i such that

$$\hat{x}_i(k) = x_i(k - d_i), \quad i = 0, 1, \dots, m-1. \quad (1)$$

In Figure 1, the general building blocks are used which have the general form depicted in Figure 2. This linear, dual-rate system is represented by $G : (p, q)$, where p and q are positive integers. This system has the (p, q) -shift invariance property in that shifting the input by q

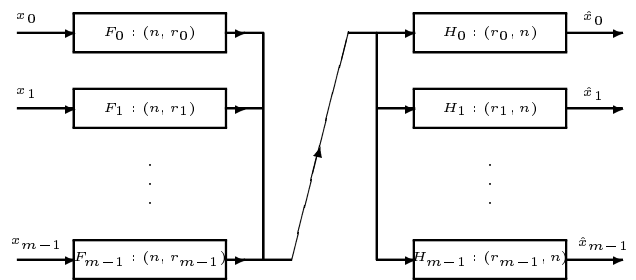


Figure 1: A nonuniform transmultiplexer using general building blocks.

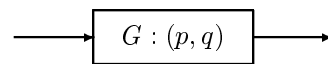


Figure 2: A dual-rate system.

samples results in shifting the output by p samples; thus the output sampling rate is p/q times the input sampling rate. Such systems allow more design freedom if p and q have nontrivial common factors; in this case, they can be implemented by the cascade combination of upsamplers, certain linear switching time-varying (LSTV) systems, and downsamplers [3].

As in the filter bank case [5, 3], perfect reconstruction is possible to achieve in Figure 1. Note that the system from x_i to \hat{x}_i is linear periodically time-varying (LPTV) with period r_i , not LTI as in the uniform case. Hence, in addition to the usual cross-talk, magnitude, and phase distortions, which are similar to the uniform case [7, 6, 4], there exists a new *aliasing distortion* from x_i to \hat{x}_i . Coping with this new distortion is effectively done later.

The paper is organized as follows. In Section 2 we develop a blocked model for the transmultiplexer in Figure 1 and relate it to the LSTV structure for implementation. Section 3 states a necessary and sufficient condition for perfect reconstruction based on the blocked model and proposes measures for cross-talk, aliasing,

¹This research was supported by the Natural Sciences and Engineering Research Council of Canada.

²Corresponding author: Telephone: (780) 492-3940; Fax: (780) 492-1811; Email: tchen@ee.ualberta.ca.

magnitude, and phase distortions, and a composite new measure. Section 4 develops an iterative design procedure for the transmultiplexer aiming at minimizing the composite distortion measure; the method is illustrated in details with a three-channel example.

2 Blocked Transmultiplexer Models

The transmultiplexer in Figure 1 can be represented by

$$T = \begin{bmatrix} H_0 \\ H_1 \\ \vdots \\ H_{m-1} \end{bmatrix} [F_0 \ F_1 \ \cdots \ F_{m-1}]. \quad (2)$$

Using the p -fold *blocking operator*, L_p , $\underline{x} = L_p x$ (underlining denotes blocking) maps to:

$$\left\{ \cdots \left| \begin{bmatrix} x(0) \\ x(1) \\ \vdots \\ x(p-1) \end{bmatrix}, \begin{bmatrix} x(p) \\ x(p+1) \\ \vdots \\ x(2p-1) \end{bmatrix}, \cdots \right. \right\}. \quad (3)$$

L_p maps ℓ to ℓp . The inverse L_p^{-1} , amounts to reversing the operation.

In view of (2), the blocked transmultiplexer, \underline{T} , is defined as follows:

$$\begin{aligned} \underline{T} &= \begin{bmatrix} L_{r_0} & & & \\ & \ddots & & \\ & & L_{r_{m-1}} & \\ & & & L_{r_{m-1}}^{-1} \end{bmatrix} T \begin{bmatrix} L_{r_0}^{-1} & & & \\ & \ddots & & \\ & & & L_{r_{m-1}}^{-1} \end{bmatrix} = \\ &= \begin{bmatrix} L_{r_0} H_0 L_n^{-1} & & & \\ \vdots & & & \\ L_{m-1} H_{m-1} L_n^{-1} \end{bmatrix} [L_n F_0 L_{r_0}^{-1} \ \cdots \ L_n F_{m-1} L_{r_{m-1}}^{-1}] \\ &= \underline{H} \underline{F}, \end{aligned} \quad (4)$$

where

$$\underline{F} = [\underline{F_0} \ \underline{F_1} \ \cdots \ \underline{F_{m-1}}], \quad (5)$$

$$\underline{H} = \begin{bmatrix} \underline{H_0} \\ \underline{H_1} \\ \vdots \\ \underline{H_{m-1}} \end{bmatrix}, \quad (6)$$

and

$$\underline{F}_i = L_n F_i L_{r_i}^{-1}, \quad \underline{H}_i = L_{r_i} H_i L_n^{-1}, \quad i = 0, 1, \dots, m-1.$$

Note \underline{T} is LTI since the shift-invariant properties of the subsystems.

We adopt the structure studied in [3] using linear switching time-varying (LSTV) systems for implementation of the general blocks in Figure 1 to compute the blocked systems $\underline{F}_i(z)$ and $\underline{H}_i(z)$.

Consider the general dual-rate system G in Figure 2 which is (p, q) -shift invariant. Write $p = l\bar{p}$ and $q = l\bar{q}$ so that l is the common factor and \bar{p} and \bar{q} are relative prime. We can represent G by the system shown in Figure 3, which involves the upsampler $\uparrow \bar{p}$, the downsampler $\downarrow \bar{q}$, l LTI systems G_0, G_1, \dots, G_{l-1} , and a periodic switch which connects each channel for $\bar{p}\bar{q}$ samples starting from time $k = 0$ and system G_0 [3]. In terms of the LTI systems G_i , the transfer matrix for $\underline{G} = L_p G L_q^{-1}$ can be computed (see Theorem 3 in [3]).

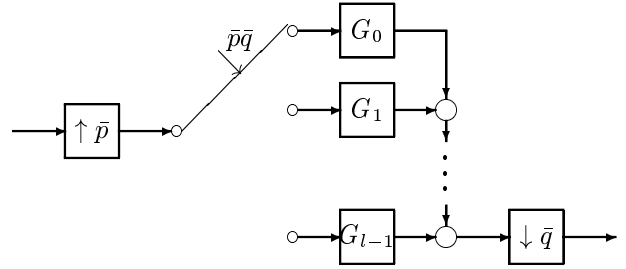


Figure 3: Implementation of a (p, q) -shift invariant system via an LSTV structure.

3 Perfect Reconstruction and Distortion Measures

As we saw in the preceding section, the blocked transmultiplexer is LTI with $\underline{T}(z) = \underline{H}(z)\underline{F}(z)$. In view of (5) and (6), we can write $\underline{T}(z)$ as a $m \times m$ block matrix:

$$\underline{T}(z) = \begin{bmatrix} T_{00}(z) & T_{01}(z) & \cdots & T_{0,m-1}(z) \\ T_{10}(z) & T_{11}(z) & \cdots & T_{1,m-1}(z) \\ \vdots & \vdots & \ddots & \vdots \\ T_{m-1,0}(z) & T_{m-1,1}(z) & \cdots & T_{m-1,m-1}(z) \end{bmatrix}, \quad (7)$$

where

$$T_{ij}(z) = \underline{H}_i(z)\underline{F}_j(z), \quad i, j = 0, 1, \dots, m-1.$$

The transmultiplexer achieves perfect reconstruction if in Figure 1 \hat{x}_i is a delayed version of x_i , i.e., if there exist nonnegative integers d_i such that $T = T_d$ with

$$T_d = \begin{bmatrix} D_{d_0} & 0 & \cdots & 0 \\ 0 & D_{d_1} & \cdots & 0 \\ \vdots & \vdots & \ddots & \vdots \\ 0 & 0 & \cdots & D_{d_{m-1}} \end{bmatrix}, \quad (8)$$

D_{d_i} being the time-delay system with transfer function $D_{d_i}(z) = z^{-d_i}$. Blocking T_d the same way as we blocked T , we can state a condition for perfect reconstruction in terms of the blocked transfer matrices.

Theorem 1 *The transmultiplexer in Figure 1 achieves perfect reconstruction iff*

$$\underline{H}(z)\underline{F}(z) = \begin{bmatrix} T_{00d}(z) & 0 & \cdots & 0 \\ 0 & T_{11d}(z) & \cdots & 0 \\ \vdots & \vdots & \ddots & \vdots \\ 0 & 0 & \cdots & T_{m-1,m-1,d}(z) \end{bmatrix},$$

where $T_{iid}(z)$ is $r_i \times r_i$ and is of the form

$$T_{iid}(z) = z^{-k_i} \begin{bmatrix} 0 & z^{-1}I_{s_i} \\ I_{r_i-s_i} & 0 \end{bmatrix} \quad (9)$$

for some integers k_i and s_i satisfying $k_i \geq 0$ and $0 \leq s_i \leq r_i - 1$. (Note that I_{s_i} is the $s_i \times s_i$ identity matrix; similarly for $I_{r_i-s_i}$.)

Proof From the previous discussion, perfect reconstruction is obtained iff for some integers d_i , \underline{T} equals the blocked T_d in (8), or equivalently,

$$\underline{H}(z)\underline{F}(z) = \begin{bmatrix} \underline{D}_{d_0}(z) & 0 & \cdots & 0 \\ 0 & \underline{D}_{d_1}(z) & \cdots & 0 \\ \vdots & \vdots & \ddots & \vdots \\ 0 & 0 & \cdots & \underline{D}_{d_{m-1}}(z) \end{bmatrix},$$

where \underline{D}_{d_i} is the blocked time-delay system $L_{r_i} D_{d_i} L_{r_i}^{-1}$. The transfer matrix for \underline{D}_{d_i} can be readily derived: Write $d_i = k_i r_i + s_i$ for $k_i \geq 0$ and $0 \leq s_i \leq r_i - 1$; then $\underline{D}_{d_i}(z)$ equals to the right-hand side of (9). The theorem is therefore proven. \square

In order to measure the degree of closeness to perfect reconstruction, we shall introduce four quantities to measure sources of distortions: cross-talk distortion, aliasing distortion, magnitude and phase distortions.

First, cross talk exists if there is any signal leakage from one channel to another, or equivalently, if there is at least one non-zero off-diagonal block in $\underline{T}(z)$. We use the 2-norm of $T_{ij}(z)$ to measure its size:

$$\|T_{ij}(z)\|_2 = \left\{ \frac{1}{2\pi} \int_0^{2\pi} \text{trace} [T_{ij}(e^{j\omega})^* T_{ij}(e^{j\omega})] d\omega \right\}^{1/2}.$$

Here $T_{ij}(e^{j\omega})^*$ is the complex conjugate transpose of $T_{ij}(e^{j\omega})$. So $\|T_{ij}(z)\|_2^2$ is the energy of this block. The energy of all the off-diagonal blocks in $\underline{T}(z)$ can be used to quantify cross-talk distortion; so we define

$$\text{CD} = \left[\sum_{i,j (i \neq j)} \|T_{ij}(z)\|_2^2 \right]^{1/2}$$

as a measure for cross-talk distortion.

If CD is zero, $\underline{T}(z)$ becomes a block-diagonal matrix; but the diagonal blocks arise from LPTV (instead of

LTI) systems in general. This fact separates the transmultiplexer in Figure 1 from the uniform ones: A new aliasing distortion may be present in the system. To quantify this effect, the following result from [2] is helpful.

Lemma 1 *An LPTV system G with period r can be uniquely decomposed into*

$$G = G^{ti} + G^{tv}$$

satisfying the two properties

(i) G^{ti} is the optimal LTI approximation of G in the sense that it minimizes $\|\underline{G}(z) - \underline{Q}(z)\|_2$ over the class of LTI Q 's [\underline{G} denotes the blocked system $L_r G L_r^{-1}$; similarly for Q].

(ii) $\|\underline{G}(z)\|_2^2 = r \|G^{ti}(z)\|_2^2 + \|G^{tv}(z)\|_2^2$.

The results in this lemma were reported in [2] using alias-component matrices; here we restated them in terms of blocked systems. The factor r in (ii) is due to the fact that we used the LTI system G^{ti} instead of \underline{G}^{ti} . How to compute this decomposition is given in [2]. Based on this lemma, the quantity $\|\underline{G}^{tv}(z)\|_2$ can be used to measure aliasing in G .

Back to our transmultiplexer problem, the system from x_i to \hat{x}_i ($H_i F_i$) is LPTV with period r_i . Thus we have

$$T_{ii}(z) = \underline{G}_i^{ti}(z) + \underline{G}_i^{tv}(z). \quad (10)$$

Aliasing distortion in the i -th channel is measured by

$$\text{AD}_i = \|\underline{G}_i^{tv}(z)\|_2. \quad (11)$$

The overall aliasing distortion is defined as

$$\text{AD} = \left(\sum_{i=0}^{m-1} \text{AD}_i^2 \right)^{1/2}. \quad (12)$$

Even if both CD and AD are zero, the i -th channel $H_i F_i$ which reduces to an LTI system G_i^{ti} may still have errors in magnitude and phase compared with the ideal time delay z^{-d_i} ; define the following quantities

$$\text{MD}_i = \left[\frac{1}{2\pi} \int_0^{2\pi} (|G_i^{ti}(e^{j\omega})| - 1)^2 d\omega \right]^{1/2}, \quad (13)$$

$$\text{PD}_i = \left\{ \frac{1}{2\pi} \int_0^{2\pi} \sin^2 [\angle G_i^{ti}(e^{j\omega}) + d_i \omega] d\omega \right\}^{1/2} \quad (14)$$

Note that MD_i and PD_i are defined across all frequencies for the i -th channel.

Next, we propose a composite distortion measure which captures all the four types of distortions and is relatively easy to use in design. Comparing the transmultiplexer T with the ideal system T_d in (8), we get the

error system $T - T_d$; the new distortion measure is the 2-norm of the blocked error transfer matrix:

$$J = \|\underline{T}(z) - \underline{T}_d(z)\|_2.$$

Such a measure is appropriate because in the next theorem we establish connections between J and the four types of distortions discussed earlier.

Theorem 2 CD , AD , and MD_i relate to J via

$$CD^2 + AD^2 + \sum_{i=0}^{m-1} r_i MD_i^2 \leq J^2; \quad (15)$$

whereas CD , AD , and PD_i relate to J via

$$CD^2 + AD^2 + \sum_{i=0}^{m-1} r_i PD_i^2 \leq J^2. \quad (16)$$

The proof of Theorem 2 requires the following lemma.

Lemma 2 Let G be a stable LTI system. Comparing $G(z)$ with the time delay z^{-d} , we have the following inequalities:

$$|G(e^{j\omega}) - e^{-jd\omega}| \geq ||G(e^{j\omega})| - 1|, \quad (17)$$

$$|G(e^{j\omega}) - e^{-jd\omega}|^2 \geq \sin^2 [\angle G(e^{j\omega}) + d\omega]. \quad (18)$$

Proof Inequality (17) follows easily. To show inequality (18), we define $\phi = \angle G(e^{j\omega}) + d\omega$ and $A = |G(e^{j\omega})|$ and note

$$|G(e^{j\omega}) - e^{-jd\omega}| = \left| |G(e^{j\omega})| e^{\angle G(e^{j\omega}) + d\omega} - 1 \right| = |Ae^{j\phi} - 1|.$$

Thus inequality (18) is equivalent to

$$\sin^2 \phi \leq |Ae^{j\phi} - 1|^2 = (A \cos \phi - 1)^2 + (A \sin \phi)^2.$$

This inequality simplifies to

$$0 \leq (A - \cos \phi)^2,$$

which is always true; and hence (18) is proven. \square

Proof of Theorem 2 From the representations for $\underline{T}(z)$ and \underline{T}_d in (7) and (8), respectively, we get

$$\underline{T}(z) - \underline{T}_d(z) = \begin{bmatrix} T_{00}(z) - \underline{D}_{d_0}(z) & \cdots & T_{0,m-1}(z) \\ T_{10}(z) & \cdots & T_{1,m-1}(z) \\ \vdots & & \vdots \\ T_{m-1,0}(z) & \cdots & T_{m-1,m-1}(z) - \underline{D}_{d_{m-1}}(z) \end{bmatrix}.$$

The first term is CD^2 . From (10) and Lemma 1 we get

$$\begin{aligned} \|\underline{T}_{ii}(z) - \underline{D}_{d_i}(z)\|_2^2 &= \|\underline{G}_i^{ti}(z) + \underline{G}_i^{tv}(z) - \underline{D}_{d_i}(z)\|_2^2 \\ &= r_i \|\underline{G}_i^{ti}(z) - z^{-d_i}\|_2^2 + \|\underline{G}_i^{tv}(z)\|_2^2 \\ &= r_i \|\underline{G}_i^{ti}(z) - z^{-d_i}\|_2^2 + AD_i^2 \end{aligned}$$

Substitute this into (??) and note (12) to get

$$J^2 = CD^2 + AD^2 + \sum_{i=0}^{m-1} r_i \|\underline{G}_i^{ti}(z) - z^{-d_i}\|_2^2. \quad (19)$$

Now by definition,

$$\|\underline{G}_i^{ti}(z) - z^{-d_i}\|_2^2 = \frac{1}{2\pi} \int_0^{2\pi} |G_i^{ti}(e^{j\omega}) - e^{-jd_i\omega}|^2 d\omega. \quad (20)$$

Invoke Lemma 2 to get

$$\begin{aligned} |G_i^{ti}(e^{j\omega}) - e^{-jd_i\omega}| &\geq ||G_i^{ti}(e^{j\omega})| - 1|, \\ |G_i^{ti}(e^{j\omega}) - e^{-jd_i\omega}|^2 &\geq \sin^2 [\angle G_i^{ti}(e^{j\omega}) + d_i\omega]. \end{aligned}$$

Combining these two equalities with (20) and noting the definitions of MD_i and PD_i in (13) and (14), we have

$$\begin{aligned} \|\underline{G}_i^{ti}(z) - z^{-d_i}\|_2 &\geq MD_i, \\ \|\underline{G}_i^{ti}(z) - z^{-d_i}\|_2 &\geq PD_i. \end{aligned}$$

The proof is complete by noting (19) and the above two inequalities. \square

In view of Theorem 2, one can define the overall magnitude and phase distortions for the transmultiplexer in Figure 1 as follows:

$$MD = \left(\sum_{i=0}^{m-1} r_i MD_i^2 \right)^{1/2}, \quad PD = \left(\sum_{i=0}^{m-1} r_i PD_i^2 \right)^{1/2}.$$

Then it is clear from Theorem 2 that all distortions (CD , AD , MD , and PD) are bounded above by J . Therefore it makes sense to minimize J in transmultiplexer design because this suboptimizes the four distortions simultaneously.

4 Design Procedure and Example

In view of Figure 1 and the new distortion measure J discussed in the preceding section, we wish to design synthesis and analysis subsystems to minimize J . The subsystems are implemented via the LSTV structure in Figure 3 with LTI systems which are FIR of a given length. Thus our optimal transmultiplexer design problem using FIR subsystems can be stated as follows:

Given the desired reconstruction time delays d_0, d_1, \dots, d_{M-1} , design FIR synthesis and analysis subsystems of some given lengths to minimize J .

Such an optimal design problem can be recast using the blocked model: Given $\underline{T}_d(z)$, design $\underline{F}(z)$ and $\underline{H}(z)$ of some given lengths to minimize

$$J = \|\underline{H}(z)\underline{F}(z) - \underline{T}_d(z)\|_2.$$

Because both $\underline{F}(z)$ and $\underline{H}(z)$ are designable, this optimization problem is in general nonlinear and difficult to solve. Thus we propose the following iterative design procedure which turns out to be very effective in the design example to follow.

Step 1 Design synthesis subsystems to satisfy desired frequency limiting properties (without considering reconstruction performance); these are used to initiate the iteration.

Step 2 Fixing the synthesis subsystems, design FIR analysis subsystems by minimizing J ; using the blocked models, this is equivalent to

$$\min_{\underline{H}(z)} \|\underline{H}(z)\underline{F}(z) - \underline{T}_d(z)\|_2.$$

Step 3 Fixing the analysis subsystems just designed, now redesign FIR synthesis subsystems by minimizing J ; using the blocked models, this is equivalent to

$$\min_{\underline{F}(z)} \|\underline{H}(z)\underline{F}(z) - \underline{T}_d(z)\|_2.$$

Step 4 Repeat Steps 2 and 3 until J is sufficiently small.

Let us now illustrate with a design example. Consider the three-channel nonuniform transmultiplexer depicted in Figure 4. This structure is interesting because it is mixed in that the synthesis part is built with traditional blocks, whereas the analysis part with general blocks. We initially use truncated and shifted

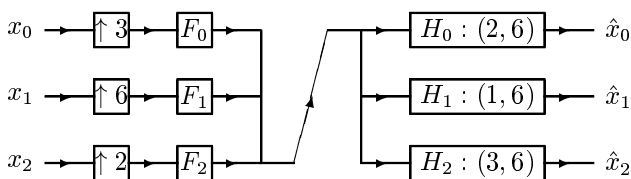


Figure 4: A three-channel nonuniform transmultiplexer using general analysis building blocks.

ideal filters to start the iterative procedure. Suppose that FIR and causal synthesis filters of order 35 are to be designed. The magnitude Bode plots of these initial synthesis filters (FIR and causal with order 35) are given in Figure 5. The general blocks for analysis are represented by the LSTV structure in Figure 3, such as, $H_0 : (2, 6)$ is implemented by an LSTV system with two LTI systems denoted by $H_{0,0}$ and $H_{0,1}$ followed by $\downarrow 3$ and so on. Thus for the analysis part, there are six LTI filters to be designed: $H_{0,0}, H_{0,1}, H_{1,0}, H_{2,0}, H_{2,1}$, and $H_{2,2}$. All the six LTI filters are causal and FIR with order 35 in the design exercise.

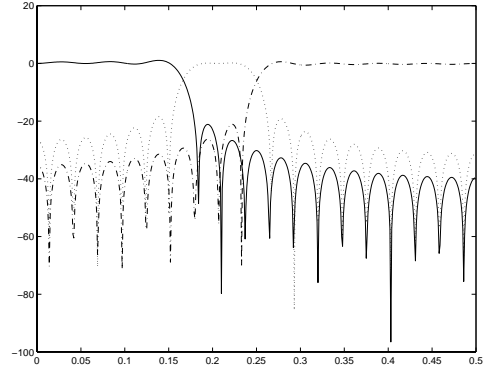


Figure 5: The magnitude Bode plots for the initial F_0 (solid), F_1 (dotted) and F_2 (dash-dot): dB versus $\omega/2\pi$

Shifting the truncated ideal filters for causality introduces time delays in the reconstruction; it is easy to calculate that these are $d_0 = 12$, $d_1 = 6$, and $d_2 = 18$, which are fixed in the design steps.

In order to have some control of the band limiting properties of the synthesis filters, in Step 3 of the iterative design procedure presented earlier we include penalties on the stopband ripples in the synthesis filters (F_0 , F_1 , and F_2) to be designed: Instead of minimizing J to design synthesis filters, we minimize the quantity

$$J^2 + \alpha_0 J_0^2 + \alpha_1 J_1^2 + \alpha_2 J_2^2,$$

where

$$J_0 = \left\{ \left[\int_{-\pi}^{-\pi/3} + \int_{\pi/3}^{\pi} \right] |F_0(e^{j\omega})|^2 d\omega \right\}^{1/2},$$

$$J_1 = \left\{ \left[\int_{-\pi}^{-\pi/2} + \int_{-\pi/3}^{\pi/3} + \int_{\pi/2}^{\pi} \right] |F_1(e^{j\omega})|^2 d\omega \right\}^{1/2},$$

$$J_2 = \left[\int_{-\pi/2}^{\pi/2} |F_2(e^{j\omega})|^2 d\omega \right]^{1/2}.$$

In our design of FIR synthesis filters of order 35, these are taken to be

$$\alpha_0 = 0.02, \quad \alpha_1 = 0.02, \quad \alpha_2 = 0.04.$$

The iterative procedure then generates a design with J converging to the value $J = 0.003050$. The Bode magnitude plots for the three synthesis filters and six analysis filters designed are given in Figures 6-9, and distortions achieved are given in Table 1. Note that the synthesis and analysis filters are band limited.

In summary, in this paper we studied a general nonuniform transmultiplexer problem. We proposed quantities to measure various distortions, among which was the aliasing distortion which is unique and new due to

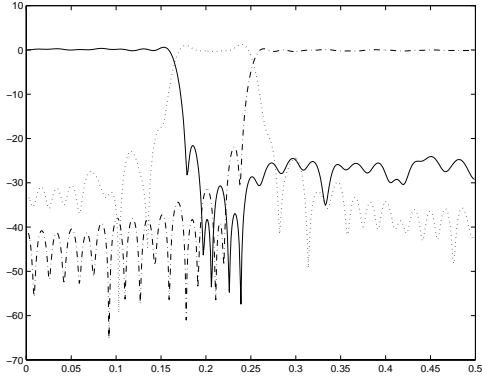


Figure 6: The magnitude Bode plots for the designed F_0 (solid), F_1 (dotted) and F_2 (dash-dot): dB versus $\omega/2\pi$

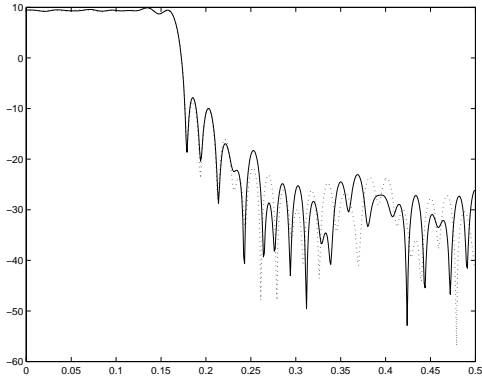


Figure 7: The magnitude Bode plots for the designed $H_{0,0}$ (solid), $H_{0,1}$ (dotted): dB versus $\omega/2\pi$

the general structures used. We also introduced a composite distortion (J) which captures all distortions. Finally, we developed an iterative design procedure based on minimizing J and successfully applied this procedure to design of a three-channel nonuniform transmultiplexer.

References

[1] T. Chen, "Nonuniform multirate filter banks: analysis and design with an H-infinity performance measure," *IEEE Trans. on Signal Processing*, vol. 45, no. 3, pp. 572-582, 1997.

J	0.003050
CD	0.001031
AD	0.001933
MD	0.0001821
PD	0.0002117

Table 1: Distortions for design using general blocks.

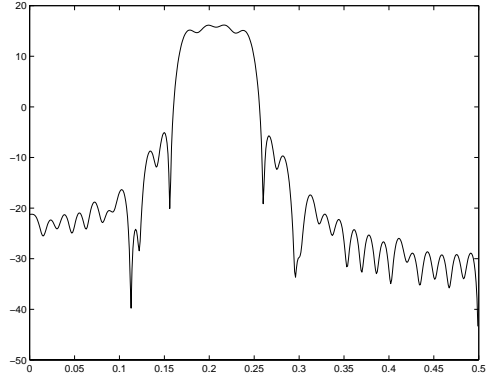


Figure 8: The magnitude Bode plots for the designed $H_{1,0}$: dB versus $\omega/2\pi$

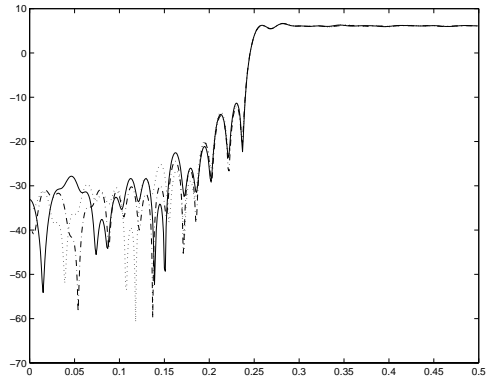


Figure 9: The magnitude Bode plots for the designed $H_{2,0}$ (solid), $H_{2,1}$ (dotted) and $H_{2,2}$ (dash-dot): dB versus $\omega/2\pi$

[2] T. Chen and L. Qiu, "Linear periodically time-varying discrete-time systems: aliasing and LTI approximations," *Systems and Control Letters*, vol. 30, pp. 225-235, 1997.

[3] T. Chen, L. Qiu, and E. Bai, "General multirate building structures with application to nonuniform filter banks," the Special Issue on Multirate Systems, Filter Banks, Wavelets, and Applications, *IEEE Trans. on Circuits and Systems II: Analog and Digital Signal Processing*, vol. 45, no. 8, pp. 948-958, 1998.

[4] T. Liu and T. Chen, "Optimal design of multi-channel transmultiplexers," accepted for publication in *Signal Processing*.

[5] R.G. Shenoy, "Multirate specifications via alias-component matrices," *IEEE Trans. on Circuits and Systems II: Analog and Digital Signal Processing*, vol. 45, pp. 314-320, 1998.

[6] P.P. Vaidyanathan, *Multirate Systems and Filter Banks*, Prentice-Hall, Englewood Cliffs, NJ, 1993.

[7] M. Vetterli, "Perfect transmultiplexers," *Proc. IEEE Int. Conf. Acoust. Speech and Signal Processing*, pp. 2567-2570, Tokyo, Japan, April 1986.